Effect of wall angle on Al 3003 strain hardening for parts formed by computer numerical control incremental forming

Article · November 2003

DOI: 10.1243/095440503771909944

CITATIONS
24

READS
1,205

2 authors:

Eric Hagan
Canadian Conservation Institute
21 PUBLICATIONS **472** CITATIONS

SEE PROFILE

Jack Jeswiet
Queen's University
131 PUBLICATIONS **5,719** CITATIONS

SEE PROFILE

Effect of wall angle on Al 3003 strain hardening for parts formed by CNC incremental forming

E Hagan and **J Jeswiet**

Department of Mechanical Engineering, Queen's University, Canada

Abstract: The change in material properties for annealed Al 3003 after CNC incremental forming was studied through a series of tensile tests. Specific shapes were designed with wall angles of 20° to 60°, in 10° increments, to allow for removal of flat specimens of adequate size. A relationship was found, with plots of stress strain curves, showing an increase in yield and necking stress for increasing wall angle. Empirical equations proposed by both Hollomon and Voce were applied to the data showing the usefulness of each method for Al 3003 formed to large strains. Strain data from previous grid measurements was used to offset the stress-strain curves, and show a tendency to follow an overall curve. A log plot of these offset curves resulted in a straight line, and therefore, a Hollomon equation was determined for Al 3003 over the full range of working strain.

Keywords: incremental forming, tensile testing, shear forming, sheet metal

NOTATION

K	Strength coefficient
k	Voce exponent
ΔL	Surface increment
n	Strain hardening exponent
R_m	True strain at necking
S_0	True yield stress at 0.05 offset true strain
S_m	True stress at necking
S_{inf}	True stress at infinite strain
σ	True stress
ΔZ	Depth increment
L-L	Along tool-path, along rolling direction
L-T	Along tool-path, across rolling direction
T-T	Across tool-path, across rolling direction
ϕ	Wall angle (blank plane to wall surface)

1 INTRODUCTION

A new manufacturing method termed CNC incremental forming was studied from a variety of different perspectives as part of a master's thesis. In short, incremental forming involves computer generation of a shape, which is then transferred into tool-path generation software. Control of the forming tool is provided by code created in MasterCAM. A file with this information is loaded onto a CNC milling machine, where a special forming tool replaces the cutter. A simple apparatus, designed for this process, sits on the mill bed, and provides support for the metal sheet during forming.

Data was collected to compliment practical applications that were studied for industry. Measurements involved surface roughness, tensile tests, strain grids, and wall angle. Roughness measurements for various depth increments were collected, which allow for knowledgeable control of the surface finish. The focus of this paper covers the change in Al 3003 material properties for increasing wall angle. Data was collected by performing tensile tests on specimens formed to various wall angles between 20 and 60 degrees.

Stress-strain curves are presented here to provide insight into the specific effect of this process on strain hardening of Al 3003-0. In addition, a detailed strain grid analysis provides the three components of strain for different amounts of deformation. These measurements allow for graphing of offset stress-strain curves to illustrate the effect of previous cold working by CNC forming.

2 TESTING METHOD

CNC incremental forming requires a 3-axis milling machine and an apparatus to hold the metal sheet during deformation. Incremental backward bulge forming, studied by both Matsubara [1] and Jeswiet [2] involves forming the convex surface of the part, which requires bushings to allow the outer perimeter to slide down. A reverse method was used here [3], requiring a fixed perimeter to form the inner surface.

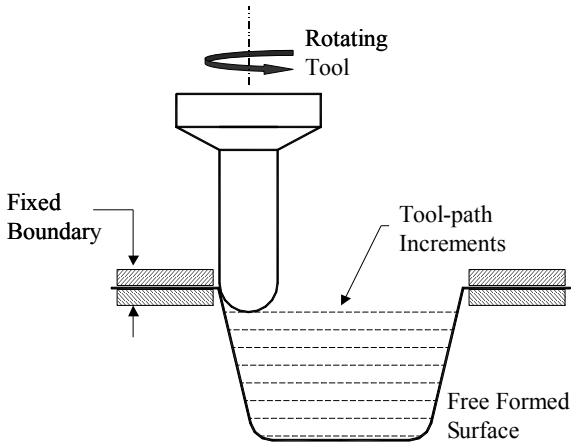

Figure 1 CNC forming of a simple cone.

The forming tool was machined from a high carbon steel rod to have a 13mm diameter hemispherical tip. Figure 1 illustrates the shape of the tool and the setup to form a simple cone. The perimeter of the sheet remains fixed while the rotating tool follows incremental tool-path contours. Tool speed was set in MasterCAM, while the RPM was controlled directly on the CNC mill. In general, the RPM was set to a value such that the tool rolled over the sheet surface. This minimized friction between the tool and work piece, and reduced the amount of heat generated. The feed rate was consistently set to a value of 25 mm/s, in which the maximum possible speed was 40mm/s. Selected speeds and feeds were controlled variables during material testing.

2.1 Test Shape

Five shapes were designed to determine changes in material properties for various amounts of deformation. The diagram in figure 2 illustrates solid models with wall angles of 20, 30, 40, and 50 degrees from the top plane. In addition, a 60^0 specimen was formed, however, it is not shown here. Each of these specimens was formed from fully annealed, 1.3mm thick, Al 3003.

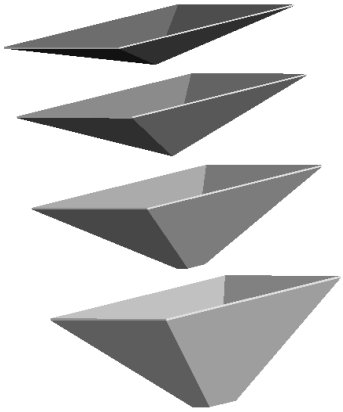

Figure 2 Solid models of tensile test shapes.

The reason behind designing such shapes was to create flat walls, which were subjected to different amounts of work hardening. These flat sections provided material for tensile testing, surface roughness measurements, and strain grid analysis. Tensile tests require flat segments, and the remaining tests are much more difficult to perform on curved sections.

2.2 Surface Roughness

Variation in surface roughness between tensile specimens was a concern when selecting the tool-path depth increment. For a constant increment the roughness varies dramatically due to the changing wall angle. With a shallow angle the tool will move along the surface further than it will for a steep wall. The depth increment was modified for each wall angle to create a similar surface finish on each specimen tested.

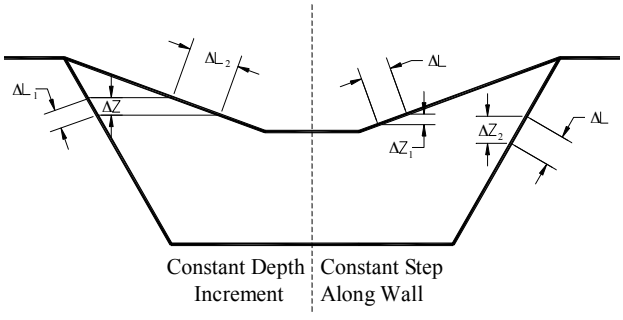

Figure 3 Relationship between depth increment, and tool motion translation along the wall surface.

Two methods of controlling the depth increments are shown in figure 3. The diagram on the left illustrates a situation in which the depth increments (ΔZ) are kept constant for two different wall angles. For this situation, surface roughness increases with decreasing wall angle measured from the top plane. The alternate situation, on the right of figure 3, involves changing the depth increment to maintain a constant step along the surface wall. Tool depth increments were set in MasterCAM according to this method for greater consistency of surface roughness. For each specimen the wall increment, ΔL, was 0.5mm with a constant feed rate of 13 mm/s. The RPM was set to a value at which the tool rolled along the surface to minimized friction.

2.3 Sample Preparation

A plasma cutter was used to remove each wall from the parts. Also, cool air was applied to the surfaces during cutting in an attempt to minimize any possibility of grain changes caused by heat generation.

Orientation of the rolling direction was noted before cutting out the specimens although the material was fully annealed from H14 stock. Samples were tested both parallel and perpendicular to the tool-path marks. Also, these tests were performed along, and across, the rolling direction. The dimensions of the specimens were obtained from the ASTM-B557M sub-size standard.

An Instron 8521 machine was used along with software, which saved load-displacement measurements for a ramp rate of 1.5 mm/min. From these data the true stress-strain curves were plotted, and empirical equations were determined using methods of both Hollomon, and Voce. These two methods will be discussed further with the analysis of collected data.

3 STRESS-STRAIN DATA

Tensile test data was collected for three different combinations of tool-path, and rolling direction. The L, and T notation refers to longitudinal and transverse direction, where the first letter is for the tool-path, and the second for rolling direction. Two samples were tested for the L-L, and T-T cases, however only one for L-T. It is important to note that duplicate samples were taken from identical specimens, and not from separate parts.

Figure 4 shows three true stress-strain curves for annealed sheet prior to incremental forming. The top two curves were along the rolling direction, while the bottom one was measured perpendicular. The middle curve was used to provide a data point on the y-axis, 0° wall angle, for all tensile test data that follow.

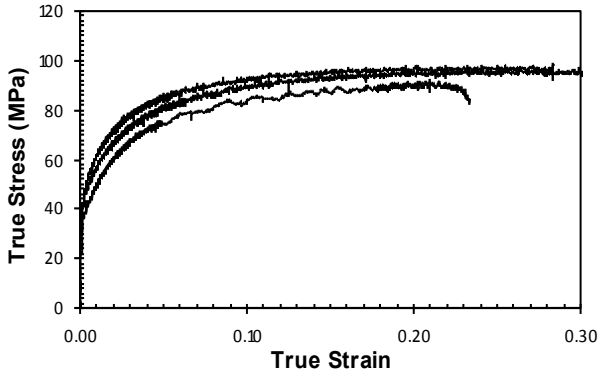

Figure 4 True stress-strain curves for fully annealed Al 3003 sheet used in forming test specimen shapes.

Data was plotted for different combinations of tool-path and rolling direction on the tensile specimens. Figure 5 illustrates the series of true stress-strain curves plotted for one of the T-T sample sets. Similar plots for each of the other four sets of data are not shown here, however, similar trends were evident.

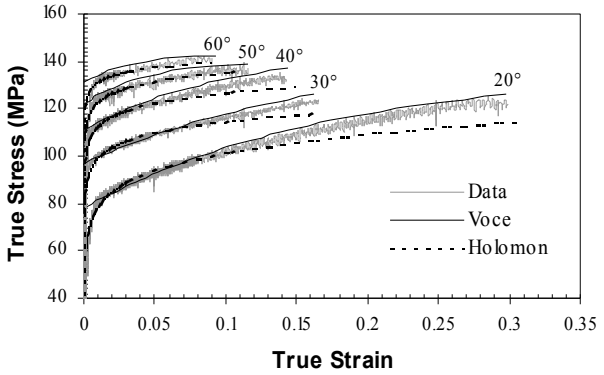

Figure 5 True stress-strain data for one of the T-T sample sets with empirical curves.

4 EMPERICAL ANALYSIS

Empirical curves determined using the methods of Hollomon and Voce are plotted along with data for each angle in figure 5. The dashed lines correspond to the Hollomon equation, which tend to fall below

the data after necking occurs. The Voce equation predicts the region beyond necking better for this material, however this method was slightly more difficult to apply. Since Al 3003 deforms in a homogeneous manner the Voce equation is better suited for predicting the stress-strain curves. Specific parameters involved in determining the empirical curves are presented next to outline the application of each method.

4.1 Hollomon Equation

A log plot of the true stress-strain curves provides a graphical means of determining the n, and K parameters of the Hollomon empirical equation. Figure 6 shows a log plot for the T-T case, where the straight trend-lines give the strain hardening exponent as the slope, and the strength coefficient as the y intercept. The fit proposed by Hollomon is given as equation 1 below.

$$\sigma = K\varepsilon^{n} \qquad \textbf{Equation 1}$$

The linear trend-lines shown for every angle in figure 6 were determined for data beginning where the linear region started, up to the necking point. Similar plots were created for each set of data giving several n, and K, values for comparison. Duplicate samples were averaged together with the results for each combination of wall angle presented in figures 7 and 8.

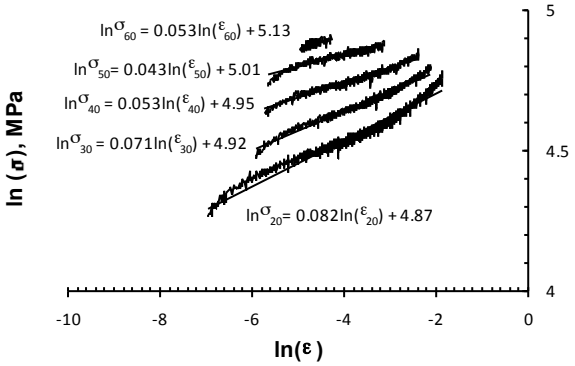

Figure 6 Ln stress-strain curves of the sample set shown in figure 5.

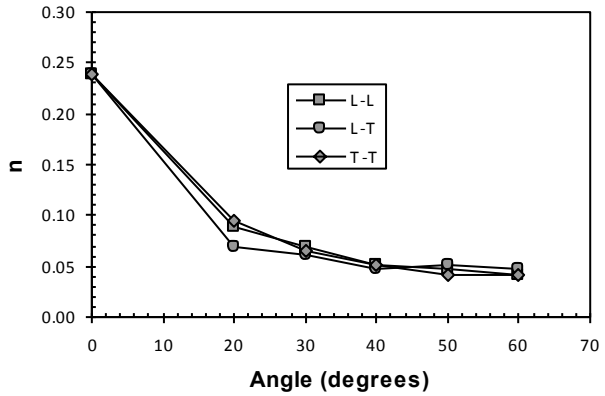

Figure 7 Strain hardening exponent determined as a function of wall angle for three combinations of tool-path and grain orientation.

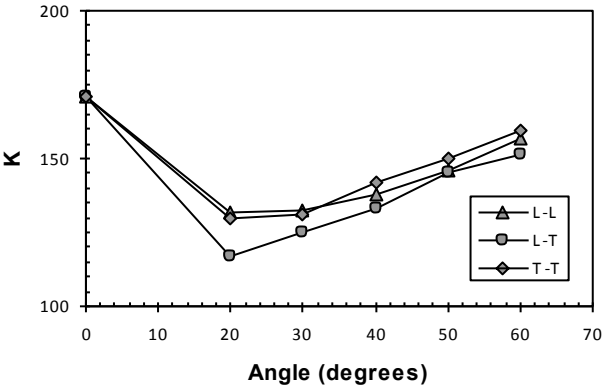

Figure 8 Strength coefficient determined as a function of wall angle for three combinations of tool-path and grain orientation.

4.2 Voce Equation

Voce [4] provides an empirical equation specifically for the condition of homogeneous deformation. This is useful for materials such as aluminum especially at high strains. As shown in figure 5 the curves tend to flatten out at higher wall angles due to large pre-strains by CNC forming. The stress asymptotically approached at infinite strain is given by equation 2 as follows:

$$S_{\inf} = (1+k)\cdot S_{m} \qquad \textbf{Equation 2}$$

Equation 2 requires the necking stress, which was determined from experimental data. The 'k' value, however, requires solving equation 3. For this research the yield stress, S_0, was found to apply well when determined at a 0.05 offset true strain.

$$R_m = \left\{ \frac{1}{k} \left(1 + k - \frac{S_0}{S_m} \right) \right\}^k \qquad \textbf{Equation 3}$$

With S_0, and S_m determined directly from experimental data, and 'k' found using equations 3, the relationship between true stress and strain was plotted according to equation 4:

$$\varepsilon = k \cdot \ln\left(\frac{S_{\inf} - S_0}{S_{\inf} - \sigma} \right) \qquad \textbf{Equation 4}$$

Three stresses S_0, S_m, and S_{inf}, are plotted together in figure 9. As expected, the stress at infinite strain, given by equation 2, is relatively constant. The difference between each of these stresses decreases for increasing angle. This is explained by flattening of the stress-strain curve at large deformation, in which the material deforms in a homogeneous manner.

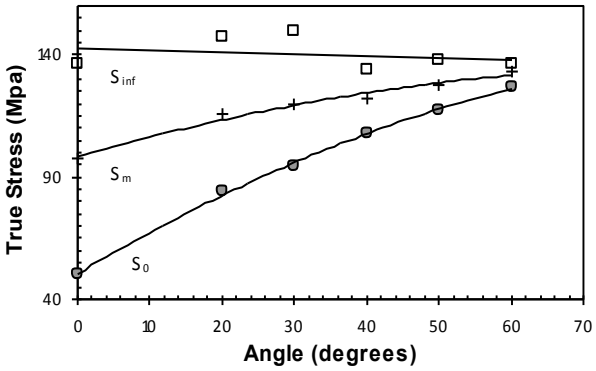

Figure 9 Stress at infinite strain, necking stress, and yielding stress as a function of wall angle.

The true strain at necking, corresponding to R_m, decreases linearly with increasing wall angle as shown in figure 10. Work hardening of the material causes necking to occur earlier at larger angles. The final parameter, 'k', used in the Voce equation is plotted in figure 11. Average values were between 0 and 0.3. The large error bars come from accumulated error from the other parameters used in equation 3.

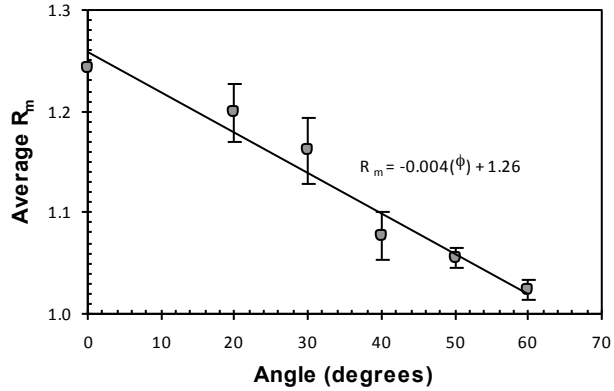

Figure 10 Average true strain at necking as a function of wall angle. Error bars show 95% confidence intervals.

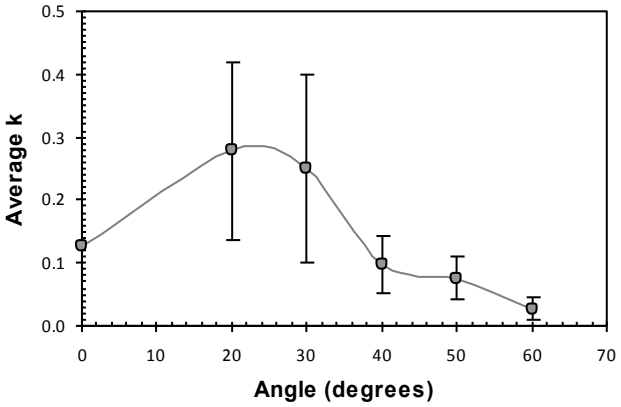

Figure 11 Average k values used in the Voce equation as a function of wall angle. Error bars show 95% confidence intervals.

5 OFFSET CURVES

A file containing a grid of 2.5mm diameter circles, spaced 3.5mm between center points was supplied to a screen-printing company along with aluminum sheets. The result was an excellent grid pattern that was accurately measured under magnification. Figure 12 illustrates the deformed grid pattern for both 60^0 and 20^0 wall angles. The original solid model is also shown to the right with corresponding axes for reference.

Strain measurements from the flat wall sections of the tensile specimen test shape were compared with expected values using the sine law given by equation 5.

$$t_f = t_i \sin\alpha \qquad \textbf{Equation 5}$$

Final thickness was determined simply with the use of a micrometer, however the remaining two strain components were determined using grid techniques. The results for all three strain components are given in figure 13 with x, y, and z being major, minor, and thickness strains respectively. Measured strains were very close to sine law calculations due to the fact that no material can flow in from the flange region. The material within the outer perimeter of the part is considered a closed system, in which the material must form primarily by simple shear to maintain constant volume. Minor strain, about the circumference of the cone, was approximately equal to zero, which gave the major strain as a mirror image of the thickness strain. Due to constant volume the sum of the strains must equal zero, therefore, if one component is negligible the other two are of equal magnitude, but opposite sign. This same distribution of strains is shown in literature for shear forming of conical shapes [5].

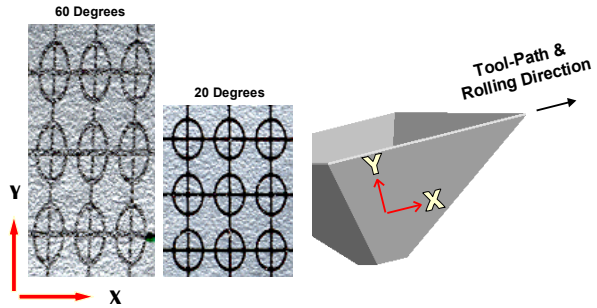

Figure 12 Illustration of strain grids from 60^0 (left) and 20^0 (right) specimens. The model on the right shows the corresponding axes for reference.

Taking the major strain results, in figure 13, and using these values to offset the true strain of stress-strain curves, at each corresponding angle, results in a series of curves shown in figure 14. For this graph the stress-strain results were averaged, and cut off at a point where the shortest of the curves ends at each respective angle.

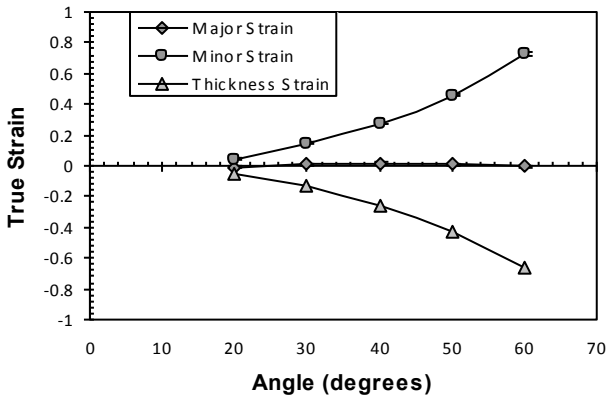

Figure 13 Measured strain components from the tensile specimen wall.

The purpose of displaying results in a manner such as figure 14 was to show the effect of previous cold working on properties of Al 3003. Theoretically, the series of curves is expected to follow an extension of the annealed curve over the entire range of strain. Offsetting averaged data shows a tendency for curves of each wall angle to follow a general trend predicted by previous deformation of the aluminum sheet. Therefore, effects of strain hardening on the wall of a CNC incrementally formed part are directly related to the wall angle. Given the wall angle, major strains are known from the sine law, and thus material properties are predictable using the offset strains.

As mentioned earlier, deviation in the results was expected to come from roughness on the surface of tensile specimens. Orange peel effect on the outer surface will have a significant effect due to the small sub-size standard used in the tests. For this reason, averaging of data was necessary, and more accurate results are possible by testing more samples followed by further statistical analysis.

Application of the Hollomon equation to offset, and averaged, data is also illustrated in figure 14. The upper curve shows the Hollomon equation determined for the annealed sheet, which is extended to cover the full working strain of the material. Below this curve, an additional Hollomon equation is presented, which was determined using a log plot of the offset, and averaged, stress-strain data.

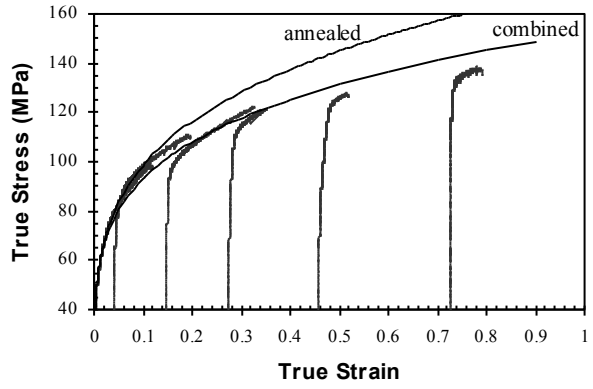

Figure 14 Stress-strain curves from figure 5 offset by major strain values shown in figure 13. Hollomon curves plotted for the annealed and offset data.

The log plot, in figure 15, illustrates that each of the offset stress-strain curves falls on a straight line. This allows for calculation of an additional Hollomon equation, which applies to the entire range of strain that the material experiences. The empirical equation for the averaged, and offset, data is shown as the lower curve in figure 14. A similar Voce equation was not determined for the offset curves due to difficulty in determining the parameters. A theoretical equation for Al 3003-0, deformed to large plastic strains, is proposed in equation 16 as follows:

$$\sigma = 152\varepsilon^{0.213} \qquad \textbf{Equation 6}$$

Where 'K' is equal to 152 Mpa, and 'n' is 0.213.

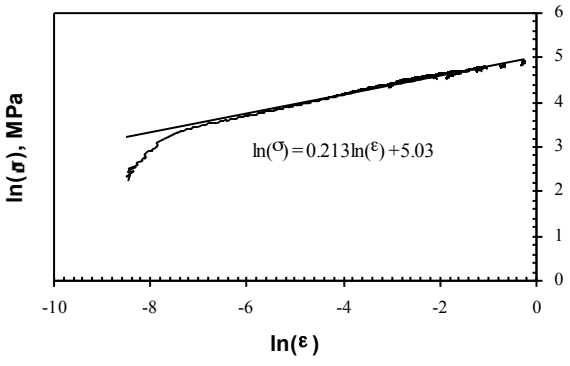

Figure 15 Log plot of the offset stress-strain curves shown in figure 14.

6 COMPARING SPECIMEN GROUPS

A comparison of experimental values for all five test samples was plotted for each angle to illustrate any trends between sets of data. The group of tensile tests for 20^0 is shown in figure 16. Sets of curves for each wall angle are not shown here due to space limitations.

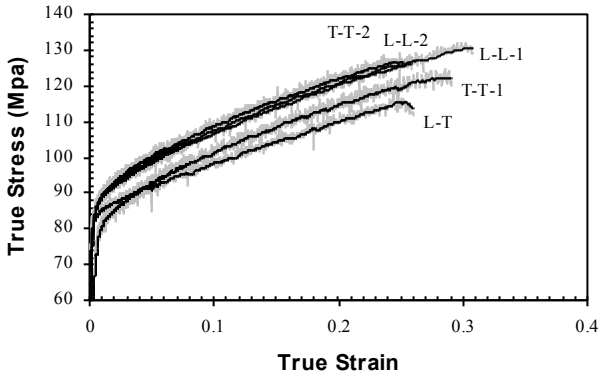

Figure 16 True stress-strain curves compared at 20^0.

The approach of this research was to show trends of material properties with respect to wall angle. A more detailed analysis would allow for the effects of rolling direction, and tool-path orientation to be accurately determined. The sample size was too small in this analysis to apply a comparison t-test to determine if there is a difference in mean values of sample data at individual angles. The results were averaged since there was not an obvious difference, thus giving a general indication of material properties at various wall angles. A series of graphs with the fives sample sets plotted together for each wall angle show some indication that the L-T stress-strain curves yield at lower stress, while the T-T curves yield somewhat higher. There is potential for future work in determining the differences in these sample sets with a more statistical analysis.

7 CONCLUSIONS

Increasing yielding and necking stresses with increasing wall angle were evident as a result of CNC forming of Al 3003. Both of these stress values approached a value of 140 Mpa at a large wall angle. This effect is predicted by Voce with an empirical equation for homogeneous deformation. In addition the necking strain was shown to decrease linearly with increasing wall angle due to strain hardening of the material.

Empirical equations of Hollomon and Voce applied well to the stress-strain data collected. The Hollomon method tended to fall below the data at

strains beyond necking. The Voce equation predicted the region beyond necking well, however, it was slightly more difficult to apply.

Stress-strain curves were offset by strains corresponding to the major strain on the deformed surface. This resulted in a series of curves, which tended to follow a general stress-strain curve. A log plot of the offset curves gave a straight line, and a Hollomon equation of $\sigma = 152\varepsilon^{0.213}$ was determined as an equation for Al 3003 deformed to large plastic strains.

A comparison of stress-strain curves for different orientations of tool-path and rolling direction did not show any obvious trends. Statistical analysis of any differences was not possible with the amount of data collected. For the purposes of this research the averaged data was sufficient to show the effects of CNC forming on Al 3003.

8 ACKNOWLEDGEMENTS

The authors thank the Center for Automotive Materials and Manufacturing for funding of this project.

9 REFERENCES

1 **Matsubara, S.** Incremental Backward Bulge Forming of a Sheet Metal with a Hemispherical Tool. *Journal of the JSTP*, vol. 35, pp. 1311-1316, 1994.

2 **Jeswiet, J.** Incremental Single Point Forming. *Proceedings of the NSF Design and Manufacturing Research Conference*, January 2000.

3 **Jeswiet, J., Hagan, E.** Rapid Proto-typing of a Headlight with Sheet Metal, Proceedings of Shelmet, April 2001, pp 165-170.

4 **Voce, E.** The relationship between stress and strain for homogeneous deformation. *J. Inst. Metals*, vol. 74, pp. 537-562, 1948.

5 **Quigley, E., Monaghan, J.** Metal forming: analysis of a spinning process. *Journal of Materials Processing Technology*. vol. 103, pp. 114-119, 2000.